Differential charge boost in hysteretic ferroelectric-dielectric heterostructure capacitors at steady state

Cite as: Appl. Phys. Lett. **118**, 122901 (2021); https://doi.org/10.1063/5.0035880 Submitted: 31 October 2020 . Accepted: 16 February 2021 . Published Online: 22 March 2021

D Nujhat Tasneem, D Prasanna Venkatesan Ravindran, D Zheng Wang, Jorge Gomez, D Jae Hur, Shimeng Yu, Suman Datta, and D Asif Islam Khan

COLLECTIONS

Paper published as part of the special topic on Ferroelectricity in Hafnium Oxide: Materials and Devices







ARTICLES YOU MAY BE INTERESTED IN

Perspective on ferroelectric, hafnium oxide based transistors for digital beyond von-Neumann computing

Applied Physics Letters 118, 050501 (2021); https://doi.org/10.1063/5.0035281

Next generation ferroelectric materials for semiconductor process integration and their applications

Journal of Applied Physics 129, 100901 (2021); https://doi.org/10.1063/5.0037617

Polarization switching in thin doped HfO₂ ferroelectric layers

Applied Physics Letters 117, 262904 (2020); https://doi.org/10.1063/5.0035100





Differential charge boost in hysteretic ferroelectric-dielectric heterostructure capacitors at steady state

Cite as: Appl. Phys. Lett. **118**, 122901 (2021); doi: 10.1063/5.0035880 Submitted: 31 October 2020 · Accepted: 16 February 2021 · Published Online: 22 March 2021







AFFILIATIONS

- School of Electrical and Computer Engineering, Georgia Institute of Technology, Atlanta, Georgia 30332, USA
- 2 School of Electrical and Computer Engineering, University of Notre Dame, Notre Dame, In 46556, USA
- ³School of Materials Science and Engineering, Georgia Institute of Technology, Atlanta, Georgia 30332, USA

Note: This paper is part of the Special Topic on Materials and Devices Utilizing Ferroelectricity in Halfnium Oxide.

a) Author to whom correspondence should be addressed: ntasneem3@gatech.edu

ABSTRACT

A ferroelectric material in a ferroelectric-dielectric heterostructure can provide a charge boost, as often discussed in the context of negative capacitance, and, in doing so, can reduce the power dissipation in field-effect transistor technology. However, there is an ongoing debate on whether the charge boost in such a heterostructure is a transient phenomenon or a steady state one. In this Letter, we use the positive-up-negative-down (PUND) measurement technique on a ferroelectric-dielectric (FE-DE) capacitor to show that the charge boost is a steady-state effect—i.e., the charge boost remains intact after the initial transient effects subside and all the voltages in the system reach constant values and steady states. We also demonstrate differential charge boost in steady state using a staircase voltage pulse measurement technique. An experimentally calibrated multi-domain SPICE model of an FE-DE stack is used to accurately simulate the PUND and staircase voltage hopping methods.

Published under license by AIP Publishing. https://doi.org/10.1063/5.0035880

A ferroelectric (FE)-dielectric (DE) heterostructure is one of the commonly used model systems to probe negative capacitance effects. In such a system, the change in charge due to a change in source voltage can be larger than the change in charge when the same change in source voltage is experienced only by the constituent DE capacitor. Such a differential charge boost, when achieved without a hysteresis, can lower the power supply voltage and the energy dissipation in a negative capacitance field-effect transistor (NCFET).

However, there has been an on-going debate as to whether the charge boost in a ferroelectric-dielectric heterostructure is a steady-state phenomenon. In this paper, we present an experiment that tests the nature of the charge boost: steady-state or transient. To that end, we study a ferroelectric-dielectric (FE-DE) heterostructure with FE Hf_{0.5}Zr_{0.5}O₂ and DE HfO₂. We utilize the well-known, positive-up-negative-down (PUND) technique where 'long' voltage pulses are applied on the FE-DE capacitor to measure its polarization vs voltage (*P*-*V*) characteristics. We performed a staircase voltage pulse measurement to find that the device under test (DUT) exhibits a differential

charge boost of steady-state nature—i.e., the charge boost remains intact after the initial transient effects subside and all the voltages in the system reach constant values and steady states. A Simulation Program with Integrated Circuit Emphasis (SPICE)-based model of the system that accounts for the multi-domain polarization switching dynamics in the FE–DE stack was also used to verify our experimental results.

According to a transient model¹⁰ of ferroelectric negative capacitance, the charge boost in an FE–DE capacitor is a consequence of (1) the mismatch between the timescales for polarization switching and the screen charge dynamics in the FE and (2) a charge imbalance between the FE and the DE. The change in the charge, ΔQ , in such a scenario is expected to be larger than that on a stand-alone dielectric [shown in Fig. 1(a)], resulting in the so-called charge boost as shown in Fig. 1(b). The fundamental aspect of the transient model is that as the screening charges balance out the polarization charges, the boost in both V_{FE} and Q diminishes to values that are expected from a series combination of two positive capacitors, thereby leading to charge

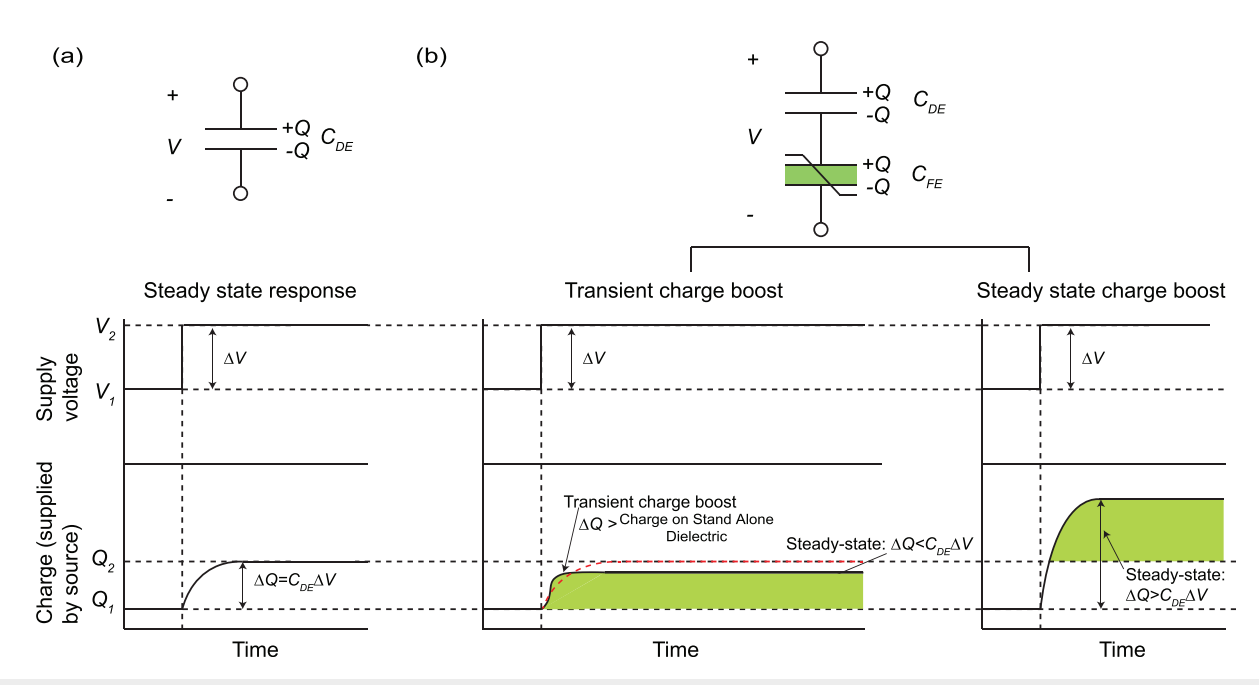


FIG. 1. Differential charge boost in a ferroelectric (FE)-dielectric (DE) heterostructure capacitor. (a) Steady characteristics of a dielectric capacitor. With a ΔV change in the source voltage, the charge across the capacitor changes by an amount $\Delta Q = C_{DE}\Delta V$ in steady state, with C_{DE} being the dielectric capacitance. (b) Differential charge boost in an FE-DE capacitor in two different scenarios: transient and steady state. In the transient model, the change in the charge across the series capacitor network increases faster than the stand-alone dielectric capacitor (shown by the red curve) but settles to a steady value $\Delta Q < C_{DE}\Delta V$, i.e., the charge boost in the FE-DE capacitor is of transient nature. In the steady state model of charge boost, the steady state change in capacitor charge is $\Delta Q > C_{DE}\Delta V$. In this Letter, we show that charge boost in an FE-DE capacitor is of steady state nature.

boost only in transience. Hence, ΔQ will be larger than the charge on the stand-alone dielectric (shown by the red curve) only for a short amount of time as shown in Fig. 1(b). Whereas if the charge boost was in fact a steady state response, then the charge boost stemming from it will prevail for the entire duration of the voltage pulse [Fig. 1(b)]. Hence, the key test for transient and steady state models of charge boost (addressed in this paper) is as follows: for a given change in voltage ΔV , is the charge supplied by the voltage source to a FE–DE capacitor ΔQ larger than $C_{DE}\Delta V$ only for a short duration of time (transient state) or an extended period of time (steady state)?

For this experiment, metal-insulator-ferroelectric-metal (MIFM) capacitors were fabricated on Si (100) substrates with a native SiO₂ layer. The bottom TiN electrode, 10 nm Hf_{0.5}Zr_{0.5}O₂ film, and the top TiN electrode (10 nm) were deposited subsequently using the plasma enhanced atomic layer deposition (PEALD) technique in a Veeco Fiji G2 Plasma ALD system with repeatable deposition of films and thickness resolution of ≤ 1 nm. The deposition was carried out at 250° C using Tetrakis(dimethylamido) hafnium, zirconium, and titanium precursors with water as the oxygen source. A post-TiN metallization annealing was done on the sample at 450° C for 30 s in a nitrogen atmosphere to crystallize the Hf_{0.5}Zr_{0.5}O₂ layer. The top TiN was then etched away using 1:1 H₂O₂, H₂O solution at 50° C. Then, 5 nm HfO2 and top TiN were grown on the films by the thermal ALD technique at 250° C. The HfO₂ layer was deposited on the already crystallized Hf_{0.5}Zr_{0.5}O₂ to avoid the rapid thermal annealing process to make sure that HfO2 remains amorphous; as a result, it will behave as a dielectric. After that, Al(100 nm) metal layers patterned into rectangular shapes were evaporated to define the capacitor areas. These evaporated Al layers also served as a hard mask during the subsequent wet etch of the top TiN electrode. The MIFM capacitor did not go through any wake-up cycling before the measurement since the effect of wakeup is not significant in these capacitors deposited via PEALD.¹¹

To accurately determine the charge-voltage characteristics, we utilized the well-known PUND method.¹² A resistor R in series with the DUT was connected to a pulse generator (supplementary material Fig. S1). An oscilloscope was used to measure voltages across the pulse generator and the DUT. To determine the ferroelectric charge, a large program pulse (V_{prog}) was first applied to fully polarize the DUT followed by two subsequent measurement pulses with varying amplitude as shown in Fig. 2(a). This 3-pulse sequence allows for the decoupling of the polarization switching (Q_{SW}) , the reversible dielectric (Q_{DE}) , and the leakage (Q_{leak}) components of the total charge. The pulses applied by the pulse generator and the measured voltage across the entire MIFM capacitor are shown in the first panel of Fig. 2(a) for $V_{prog} = -8$ V and subsequent measurement pulses of +7.4 V. An important consideration in this method is that the duration of pulses is set long enough [4 μ s, Fig. 2(a) and 1.5 μ s, Fig. S2] such that the DUT reaches steady state—i.e., the measured Q_{SW} does not have any transient contribution and corresponds to their respective steady state values. We can see from the first panel of Fig. 2(a) that the measured voltage V_{FE+DE} reaches applied voltage V_{in} at the end of each voltage pulse—an indication of steady state. This is further confirmed by the current flowing through the resistor R, which is plotted as a function of time as shown in the second panel of Fig. 2(a). The current becomes zero at the end of each applied pulse, which proves that the DUT

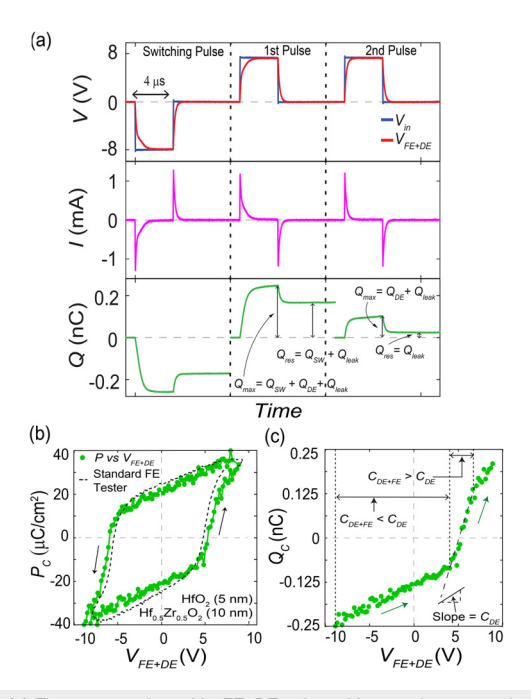


FIG. 2. (a) The source voltage V_{lm} , FE–DE voltage V_{FE+DE} , the current through R, the charge supplied by the source, Q plotted as a function of time for $V_{prog} = -8$ V, and subsequent measurement pulses of +7.4 V. The program pulse is applied before every measurement. The first measurement pulse captures Q_{SW} and Q_{DE} , while the second captures only Q_{DE} . (b) P-V curve from the PUND method (green curve) for 10 nm $Hf_{0.5}Zr_{0.5}O_2$ with 5 nm HfO_2 , overlaid on the P-V curve measured using a standard FE tester (black dotted curve). (c) Differential NC-based capacitance enhancement is shown using the PUND method.

approaches steady state. The charge supplied to the DUT is also plotted as a function of time in the third panel of Fig. 2(a). In the transient charge waveform, two significant charge points are extracted after each three-pulse sequence: the maximum charge stored on the capacitor $Q_{max}(=Q_{SW}+Q_{DE}+Q_{leak})$ from the first measurement pulse and the residual charges on the capacitor after the current approaches zero, from the second measurement pulse, which contains only leakage Q_{leak} [Fig. 2(a)]. The difference between these two gives the charge across the capacitors, $Q_C(=Q_{SW}+Q_{DE})$. An MIFM capacitor where the dielectric layer stabilizes the negative capacitance region of the ferroelectric layer has been used here to explore the nature of this region.² The polarization, $P_C(=Q_C/\text{Area of the capacitor})$, for such a capacitor as a function of $V_{max} (= V_{FE+DE})$ is shown in Fig. 2(b). The hysteretic P-V curve shown in Fig. 2(b) is superimposed on the same curve measured using a conventional FE tester (black dotted curve). While the P-V curves obtained using both the methods have approximately the same shape, the result obtained using the PUND method reflects the true steady state response of the FE-DE capacitor. Figure 2(c) demonstrates the capacitance enhancement leading to the charge boost obtained using the PUND method. It should be noted here that the 4 μ s pulse width (PW), required for the DUT to reach steady state, is long compared to the PW used in Refs. 3 and 6 (0.4-0.5 µs). This might have led to charge injection at the ferroelectric/dielectric interface and resulted in the hysteretic $P_C - V_{FE}$ curve shown in supplementary material Sec. IV, Fig. S4.

To determine the steady state response of the FE-DE capacitor to a differential voltage, we applied a staircase pulse: $5\,\mathrm{V} \to 6.5\,\mathrm{V}$ \rightarrow 8 V. Figure 3(a) shows the source voltage V_{in} , FE-DE voltage V_{FE+DE} , the current through R, and the charge supplied by the source Q as a function of time t. Note here again that the duration of each step voltage is long enough that the system reaches steady state where $V_{FE+DE} = V_{in}$ and iR = 0 at the end of each voltage pulse. Interestingly, the charge supplied during the $5 \text{ V} \rightarrow 6.5 \text{ V}$ pulse step, $\Delta Q = 0.11$ nC, is larger than $C_{DE}\Delta V$, where $\Delta V = (6.5 - 5)$ = 1.5 V ($C = \epsilon_o \epsilon_{HfO}$, A/d_{HfO} , = 18.1 pF and ϵ_{HfO} , = 20). This steady state charge boost can also be expressed in terms of capacitance enhancement shown in Fig. 2(c). It can be seen from Fig. 2(c) that for V_{FE+DE} below \sim 5 V, the slope of the $Q_C-V_{\rm max}$ curve, which corresponds to the capacitance of the MIFM heterostructure, is nearly a constant. For larger voltage pulses, the slope increases, and therefore, the capacitance increases. Until $V_{FE+DE} \approx 7$ V, the capacitance of the FE-DE layer is greater than the dielectric capacitance $(C_{FE+DE} > C_{DE})$. This capacitance enhancement in the MIFM capacitor heterostructure is due to the hafnia-zirconia FE layer since the capacitance of the dielectric HfO2 is constant with respect to the voltage across the dielectric layer (supplementary material Fig. S3). To further verify the accuracy of the staircase response, the path of (Q, V_{FE+DE}) in the time domain is overlaid on the steady state Q-Vplot in Fig. 3(b). It is clearly observed that with the application of a staircase pulse, the system hops between points on the steady state curve and the shape of the time trace is determined by the external resistor. The capacitance enhancement ($C_{FE+DE} > C_{DE}$) indicates that the capacitance of the FE layer is negative in that operating region, which is further confirmed in Fig. 3(c). Under the assumption that the capacitance of HfO2 is constant (supplementary material Fig. S3) and the negative capacitance region is stabilized in an FE-DE capacitor, we extracted the voltages across the FE layer V_{FE} and plotted its $Q - V_{FE}$

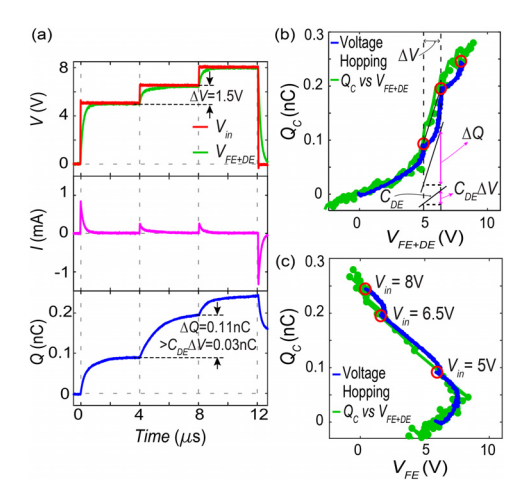


FIG. 3. (a) Staircase pulse: $5\,\mathrm{V} \rightarrow 6.5\,\mathrm{V} \rightarrow 8\,\mathrm{V}$ of time period 4 $\mu\mathrm{s}$ is applied to the FE–DE heterostructure to analyze the nature of differential charge boost. (b) Charge boost is shown in the charge–voltage characteristics of the FE–DE heterostructure. With the application of a staircase pulse, the system hops between points on the steady state Q–V curve (green). (c) Extracted P–V characteristics of the ferroelectric layer are shown. It can be noted that the ferroelectric operates in a region with a negative slope, which leads to the observed charge boost and capacitance enhancement in the FE–DE heterostructure.

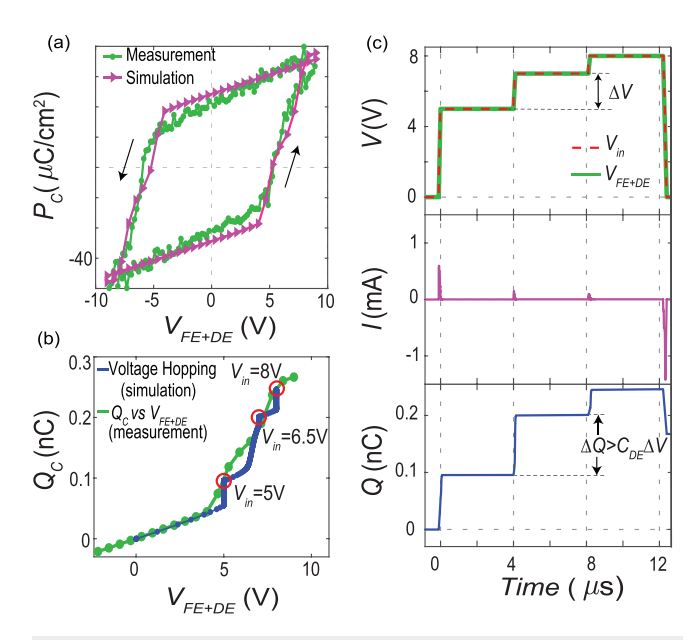


FIG. 4. (a) Simulated (pink) and experimental (green) P–V curve for the FE–DE heterostructure. (b) Simulated (blue) points for staircase pulse overlaid on the experimental (green) Q–V curve. (c) Simulated staircase pulse time plots.

characteristics [Fig. 3(c)]. This experimental $Q-V_{FE}$ curve reveals that the ferroelectric operates in a region with a negative slope, which leads to the observed charge boost and capacitance enhancement in the FE–DE heterostructure.

A circuit-based SPICE model (supplementary material Fig. S6) incorporating a distribution of domains to emulate a multidomain FE layer was used to simulate the PUND technique and staircase pulses. The model was calibrated with experimental results by considering the device geometry and measured hysteretic P-V loops. It can be observed from Fig. 4(a) that the simulated and experimentally measured steady state polarization vs voltage loop of the FE–DE stack is in good agreement. The staircase pulses simulated using the SPICE model demonstrate voltage amplification as seen experimentally [Fig. 4(b)]. Similar to Fig. 3(b), the resulting charge and voltage points trace out the experimental steady state $Q_C - V$ plot of the FE–DE stack [Fig. 4(b)]. The simulated staircase pulse-time plots are shown in Fig. 4(c).

In summary, the results obtained from the PUND technique and the staircase pulse experiment on an FE-DE structure reveal that the charge boost in a hysteretic FE-DE structure is prevalent for the entire pulse duration and, hence, a steady state response. The experimental results match with the predictions based on a multi-domain ferroelectric model eliciting the importance of domain dynamics in obtaining the ideal stabilized negative capacitance. Investigating NCFETs and

NC Capacitors using this method will provide more insight into the charge dynamics of the systems, which can be used to advance the designs and study the physics of these devices.

See the supplementary material for experimental details, time plots of PUND measurements on the MFM capacitor, the dielectric constant of the hafnia capacitor, the extracted $P_C - V_{FE}$ loop from Fig. 2(b), P-V loop and capacitance enhancement for shorter pulses, and the SPICE model used for simulation of the FE–DE heterostructures.

AUTHORS' CONTRIBUTIONS

N.T. and P.V.R. contributed equally to this work.

This work was supported in part by the Semiconductor Research Corporation (SRC)–Global Research Collaboration program and in part by the National Science Foundation (Grant No. 1718671). This work was performed at the Georgia Tech Institute for Electronics and Nanotechnology, a member of the National Nanotechnology Coordinated Infrastructure (NNCI), which is supported by the National Science Foundation (ECCS-1542174).

DATA AVAILABILITY

The data that support the findings of this study are available within this article and its supplementary material.

REFERENCES

¹S. Salahuddin and S. Datta, Nano Lett. **8**, 405 (2008).

²A. Islam Khan, D. Bhowmik, P. Yu, S. Joo Kim, X. Pan, R. Ramesh, and S. Salahuddin, Appl. Phys. Lett. **99**, 113501 (2011).

³M. Hoffmann, F. P. Fengler, M. Herzig, T. Mittmann, B. Max, U. Schroeder, R. Negrea, P. Lucian, S. Slesazeck, and T. Mikolajick, Nature 565, 464 (2019).

⁴P. Zubko, J. C. Wojdeł, M. Hadjimichael, S. Fernandez-Pena, A. Sené, I. Luk'yanchuk, J.-M. Triscone, and J. Íñiguez, Nature 534, 524 (2016).

⁵D. J. Appleby, N. K. Ponon, K. S. Kwa, B. Zou, P. K. Petrov, T. Wang, N. M. Alford, and A. O'Neill, Nano Lett. 14, 3864 (2014).

⁶Y. J. Kim, H. Yamada, T. Moon, Y. J. Kwon, C. H. An, H. J. Kim, K. D. Kim, Y. H. Lee, S. D. Hyun, M. H. Park *et al.*, Nano Lett. **16**, 4375 (2016).

⁷M. Hoffmann, S. Slesazeck, U. Schroeder, and T. Mikolajick, Nat. Electron. 3, 504 (2020).

⁸A. Nourbakhsh, A. Zubair, S. Joglekar, M. Dresselhaus, and T. Palacios, Nanoscale 9, 6122 (2017).

⁹M. A. Alam, M. Si, and P. D. Ye, Appl. Phys. Lett. 114, 090401 (2019).

¹⁰K. Ng, S. J. Hillenius, and A. Gruverman, Solid State Commun. **265**, 12 (2017).

¹¹J. Hur, N. Tasneem, G. Choe, P. Wang, Z. Wang, A. I. Khan, and S. Yu, Nanotechnology 31, 505707 (2020).

12T. Schenk, S. Mueller, U. Schroeder, R. Materlik, A. Kersch, M. Popovici, C. Adelmann, S. Van Elshocht, and T. Mikolajick, in *Proceedings of the European Solid-State Device Research Conference (ESSDERC)* (IEEE, 2013), pp. 260–263.

¹³J. Gomez, S. Dutta, K. Ni, J. Smith, B. Grisafe, A. Khan, and S. Datta, in 2019 IEEE International Electron Devices Meeting (IEDM) (IEEE, 2019), pp. 7–1.